Localization of avalanche victims using robocentric SLAM

Pedro Piniés, Juan D. Tardós, José Neira
Instituto de Investigación en Ingeniería de Aragón (I3A)
Universidad de Zaragoza
María de Luna 1, E-50018, Zaragoza, Spain
e-mail: {ppinies, tardos, jneira }@unizar.es

***Abstract*— A person buried by a snow avalanche can be found by measuring the magnetic field generated by an avalanche beacon or ARVA carried by the victim. However, the signals received are difficult to interpret and require people with good training on the actual searching techniques. In this paper we show that the search can be automated using SLAM techniques. The rescuer is equipped with an inertial sensor to estimate its own motion and a triple antenna to obtain 3D measurements of the magnetic field generated by the victim's ARVA. Both measurements are used to build a "robocentric" map that contains the location of the victim relative to the rescuer. To solve this highly non-linear SLAM problem we propose and compare two alternative solutions based on a sum of Gaussinas (SOGs) filter and a Particle filter. We present simulation results showing that, for comparable computing times, the SOGs solution gives more accurate results.**

I. Introduction

Time is essential when rescuing people buried in the snow by an avalanche: during the first 15 minutes, a victim is found alive with a 93% of probability whereas this probability falls to 25% after 45 minutes [1]. The most useful device to localize the victims is an avalanche beacon or ARVA (*Appareil de recherche de Victimes d'Avalanche*). An ARVA is a transceiver that generates an oscillating magnetic field of $457kHz$ whose characteristics are defined on the standard *ETS 300718*. If an avalanche occurs and buries completely one or more victims, the rescuers must switch their ARVAs to reception mode and search the avalanche area trying to detect the magnetic field of the victim's ARVA and finding its location. To be successful, rescuers must be trained on the basic search techniques, briefly explained in [2]. Even for trained rescuers, there are some challenging situations such as deep burials or multiple close victims that may cause confusion and delay the rescue.

Our objective is to develop new localization techniques to automate and speed up the search. In this paper we show that finding the victims can be seen as a SLAM problem [3],[4], where the rescuer takes the role of the robot and the victims are the features to be mapped. The observations are measurements of the magnetic field vector generated by the victim's ARVAs taken with a 3D antenna carried by the rescuer. Preliminary work was presented in [2], assuming that the trajectory of the rescuer was perfectly known. Here we generalize the results to the full SLAM problem, where only imprecise information about the rescuer motion is available.

In classical SLAM the map contains the location of the robot and the environment features relative to a fixed reference. In our application we want to estimate the location of the victims relative to the rescuer. Although this information could be computed from an absolute map when needed [3], it seems more natural to build a map relative to the rescuer using *robocentric SLAM* [5]. This technique has the additional advantage of reducing the effects of linearization errors.

The main difficulty for solving this SLAM problem is the high non-linearity of the magnetic field measurement equation. As a result, the pdf describing the estimated location of a victim after a few measurements is far from being Gaussian and linear estimation techniques as the EKF become useless. In this paper we propose and compare two solutions based on a Sum of Gaussians filter [6] and on a particle filter [7].

The rest of the paper is structured as follows. Section II presents the robocentric SLAM equations used to describe the problem. In section III a solution based on the SOGs filter is proposed. Section IV discusses different approaches to the problem using particle filters. Finally, section V presents comparative simulation showing the results obtained by both methods.

II. Robocentric Mapping

In the robotic SLAM literature the map is usually built with respect to an absolute reference frame which generally coincides with the initial location of the robot. However, in this SLAM application, it is more natural to represent the location of the transmitters (map) with respect to the current location of the receiver (robot). This information and its uncertainty can be directly used to guide the rescuer to approach and find the victims. Therefore, our SLAM implementation will be based on the Robocentric Mapping [5]. An additional advantage of this technique is that reduces the effects of the linearization on the quality of the stochastic map.

In this work, two main reference frames are used. The first one is a local geographic reference frame G with its x axis pointing North, y axis pointing West and z axis pointing up, centered at the receiver's position. The second one is a reference frame R attached to the receiver's antenna and it is used to represent the components of the magnetic field measured. Its origin coincides with that of the geographic frame and its axis are aligned with the three coils of the

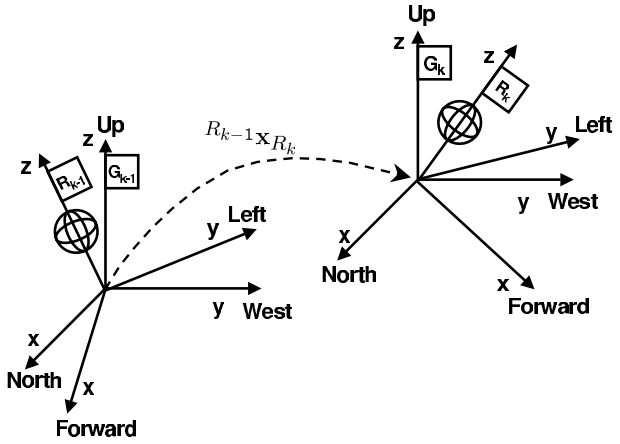

Fig. 1. Relation between local Geographic frame and Receiver frame after a movement

antenna. We assume that the x axis points to the rescuer's forward direction, the y axis points to the rescuer's left and the z axis points upwards.

The stochastic state vector used represents the location of the receiver and the transmitters in the local geographic reference:

$$\hat{\mathbf{x}}_k = \begin{bmatrix} {}^{G_k}\hat{\mathbf{\Psi}}_{R_k} \\ {}^{G_k}\hat{\mathbf{x}}_{T_1} \\ \vdots \\ {}^{G_k}\hat{\mathbf{x}}_{T_n} \end{bmatrix} ; \; \mathbf{P}_k = \begin{bmatrix} \mathbf{P}_{R_k} & \cdots & \mathbf{P}_{R_k T_n} \\ \vdots & \ddots & \vdots \\ \mathbf{P}_{T_n R_k} & \cdots & \mathbf{P}_{T_n} \end{bmatrix} \quad (1)$$

where ${}^{G_k}\hat{\mathbf{\Psi}}_{R_k} = \left[\hat{\psi}, \hat{\theta}, \hat{\phi}\right]^T$ are the roll , pitch and yaw angles which define the orientation of the receiver antenna with respect to the geographic frame. The corresponding rotation matrix is given by:

$${}^{G_k}R_{R_k} = Rot(z, \hat{\phi}) Rot(y, \hat{\theta}) Rot(x, \hat{\psi}) \quad (2)$$

The nth transmitter is described by its position in cartesian coordinates, and its magnetic moment vector, that encloses the information about the orientation and power of its antenna:

$${}^{G_k}\hat{\mathbf{x}}_{T_n} = \begin{bmatrix} {}^{G_k}\hat{\mathbf{p}}_{T_n} \\ {}^{G_k}\hat{\mathbf{m}}_{T_n} \end{bmatrix} \quad (3)$$

The basic steps of the robocentric SLAM algorithm are detailed next. For the rest of the paper, a unique transmitter will be assumed.

A. Receiver motion

A set of sensors attached to the antenna can provide the information required to estimate the antenna orientation with respect to the geographic frame and its displacement because of the rescuer's movement. The vector which describes the transformation between two consecutive receiver locations (figure 1) is:

$$\begin{aligned} {}^{R_{k-1}}\mathbf{x}_{R_k} &= \begin{bmatrix} {}^{R_{k-1}}\mathbf{p}_{R_k} \\ {}^{R_{k-1}}\mathbf{\Psi}_{R_k} \end{bmatrix} \\ &= {}^{R_{k-1}}\hat{\mathbf{x}}_{R_k} + \mathbf{w}_k \quad (4) \\ \mathbf{w}_k &\sim N(\mathbf{0}, Q_k) \end{aligned}$$

where ${}^{R_{k-1}}\mathbf{p}_{R_k}$ is the translation component and ${}^{R_{k-1}}\mathbf{\Psi}_{R_k}$ is the rotation component. The motion ${}^{R_{k-1}}\hat{\mathbf{x}}_{R_k}$ estimated has an associated process noise covariance Q_k.

The components of the state vector $\mathbf{x}_k$ in the new reference frame G_k can be calculated using the displacement as follows:

$${}^{G_k}\mathbf{\Psi}_{R_k} = {}^{G_{k-1}}\mathbf{\Psi}_{R_k} = {}^{G_{k-1}}\mathbf{\Psi}_{R_{k-1}} \oplus {}^{R_{k-1}}\mathbf{\Psi}_{R_k} \quad (5)$$

or in rotation matrix terms

$${}^{G_k}R_{R_k} = {}^{G_{k-1}}R_{R_k} = {}^{G_{k-1}}R_{R_{k-1}} \; {}^{R_{k-1}}R_{R_k} \quad (6)$$

where the $\oplus$ operator represents the composition of rotations as described in [8].

The vector $\mathbf{p}_{T_1}$ that describes the position of the transmitter with respect to the current geographic reference frame can be easily obtained by:

$${}^{G_k}\mathbf{p}_{T_1} = {}^{G_{k-1}}\mathbf{p}_{T_1} - {}^{G_{k-1}}R_{R_{k-1}} \cdot {}^{R_{k-1}}\mathbf{p}_{R_k} \quad (7)$$

where $({}^{G_{k-1}}R_{R_{k-1}} \cdot {}^{R_{k-1}}\mathbf{p}_{R_k})$ is the vector that goes from the origin of the reference G_{k-1} to the origin of G_k expressed in G_{k-1} coordinates.

Finally, the magnetic moment $\mathbf{m}_{T_1}$ does not change when going from G_{k-1} to G_k since its pointing direction and modulus are the same in both references:

$${}^{G_k}\mathbf{m}_{T_1} = {}^{G_{k-1}}\mathbf{m}_{T_1} \quad (8)$$

Equations (5, 7, 8) can be condensed in a unique function $\mathbf{f}$, called composition equation which gives the new state vector after a movement:

$$\begin{aligned} \mathbf{x}_k &= \mathbf{f}(\mathbf{x}_{k-1}, {}^{R_{k-1}}\mathbf{x}_{R_k}) \\ &= \begin{bmatrix} {}^{G_{k-1}}\mathbf{\Psi}_{R_{k-1}} \oplus {}^{R_{k-1}}\mathbf{\Psi}_{R_k} \\ {}^{G_{k-1}}\mathbf{p}_{T_1} - {}^{G_{k-1}}R_{R_{k-1}} \cdot {}^{R_{k-1}}\mathbf{p}_{R_k} \\ {}^{G_{k-1}}\mathbf{m}_{T_1} \end{bmatrix} \quad (9) \end{aligned}$$

B. The prediction step

In the robocentric approach the composition equation is postponed until the composition step. Instead, the displacement vector ${}^{R_{k-1}}\mathbf{x}_{R_k}$ is included, with its corresponding covariance $\mathbf{Q}_k$ and correlation with the state $\mathbf{C}_k$, in the stochastic vector $\mathbf{x}_{k-1}$:

$$\hat{\mathbf{x}}^*_{k|k-1} = \begin{bmatrix} \hat{\mathbf{x}}_{k-1} \\ {}^{R_{k-1}}\hat{\mathbf{x}}_{R_k} \end{bmatrix} \quad (10)$$

$$\mathbf{P}^*_{k|k-1} = \begin{bmatrix} \mathbf{P}_{k-1} & \mathbf{C}_k \\ \mathbf{C}_k & \mathbf{Q}_k \end{bmatrix} \quad (11)$$

where superscript $*$ will denote the state vector augmented with the inclusion of the displacement.

Postponing the composition, the estimated relative movement will be first improved in the estimation step of the EKF reducing the effects of the linearization in the process equation.

C. The estimation step

The components of the magnetic field with respect to an arbitrary reference frame can be obtained in any position of the space from [2]:

$$\mathbf{H} = \frac{1}{4\pi r^5} \quad A \quad \mathbf{m} \tag{12}$$

$$A = \begin{pmatrix} 2r_x^2 - r_y^2 - r_z^2 & 3r_x r_y & 3r_x r_z \\ 3r_x r_y & 2r_y^2 - r_x^2 - r_z^2 & 3r_y r_z \\ 3r_x r_z & 3r_y r_z & 2r_z^2 - r_x^2 - r_y^2 \end{pmatrix} \tag{13}$$

where $\mathbf{r} = \mathbf{p}_R - \mathbf{p}_T$ is the radio vector that goes from the transmitter to the receiver. In this equation $\mathbf{r}$ and $\mathbf{m}$ must be expressed in coordinates of the reference frame selected.

The measurement equation is:

$$\begin{aligned} {}^{R_k}\mathbf{z}_k &= \mathbf{h}_k(\mathbf{x}^*_{k|k-1}) + \mathbf{v}_k \\ \mathbf{h}_k(\mathbf{x}^*_{k|k-1}) &= {}^{R_k}R_{G_k}\,{}^{G_k}\mathbf{H} \\ \mathbf{v}_k &\sim N(\mathbf{0}, R_k) \end{aligned} \tag{14}$$

where ${}^{G_k}\mathbf{H}$ are the components of the magnetic field in reference G_k, ${}^{R_k}R_{G_k}$ is the rotation matrix associated with ${}^{R_k}\mathbf{\Psi}_{G_k}$ and $\mathbf{v}_k$ is the measurement noise.

Using this measurement, a new state estimate can be obtained with the classical EKF update equations. The new state vector and its covariance are denoted by $\hat{\mathbf{x}}^*_{k|k}$ and $P^*_{k|k}$.

D. The composition step

Finally the original size of the state vector is obtained again modifying its components by the improved displacement vector. To obtain the original state vector and its covariance the composition equation evaluated in the new estimates is applied:

$$\begin{aligned} \hat{\mathbf{x}}_k &= \mathbf{f}_k(\hat{\mathbf{x}}^*_{k|k}) \\ P_k &= F_k P^*_{k|k} F_k^T \end{aligned} \tag{15}$$

where $F_k = \left.\frac{\partial \mathbf{f}_k}{\partial \mathbf{x}^*_k}\right|_{(\hat{\mathbf{x}}^*_{k|k})}$

III. SOGs Filter

We know from [2] that the posterior pdf $p(\mathbf{x}_k|Z^k)$ associated with this problem is multimodal during the initial steps of the localization. Therefore, the standard Kalman filter equations as defined in the previous section cannot be directly implemented in this case. The error in the approximation of the posterior by a unimodal gaussian distribution would be excessive. In this paper two methods are proposed to improve the approximation. The first one is based on the sum of gaussians filter (SOGs) and it is discussed in this section, the second one is based on the particle filter and it is explained on section IV.

Algorithm 1 : SOGs Filter.

for $i = 1$ to N **do**

Prediction Step:

$\hat{\mathbf{x}}^{*(i)}_{k|k-1} = \begin{bmatrix} \hat{\mathbf{x}}^{(i)}_{k-1} \\ R_{k-1}\hat{\mathbf{x}}_{R_k} \end{bmatrix}$

$P^{*(i)}_{k|k-1} = \begin{bmatrix} P^{(i)}_{k-1} & C_k \\ C_k & Q_k \end{bmatrix}$

Estimation Step:

$H_k = \left.\frac{\partial \mathbf{h}_k}{\partial \mathbf{x}^*_k}\right|_{(\hat{\mathbf{x}}^{*(i)}_{k|k-1})}$

$K_k = P^{*(i)}_{k|k-1} H_k^T (H_k P^{*(i)}_{k|k-1} H_k^T + R_k)^{-1}$

$\hat{\mathbf{x}}^{*(i)}_{k|k} = \hat{\mathbf{x}}^{*(i)}_{k|k-1} + K_k(\mathbf{z}_k - \mathbf{h}_k(\hat{\mathbf{x}}^{*(i)}_{k|k-1}))$

$P^{*(i)}_{k|k} = (I - K_k H_k) P^{*(i)}_{k|k-1}$

$w^{(i)}_k = \eta\ w^{(i)}_{k-1}\ N(\mathbf{z}_k; \mathbf{h}_k(\hat{\mathbf{x}}^{*(i)}_{k|k-1}), H_k P^{*(i)}_{k|k-1} H_k^T + R_k)$

Composition Step:

$F_k = \left.\frac{\partial \mathbf{f}_k}{\partial \mathbf{x}^*_k}\right|_{(\hat{\mathbf{x}}^{*(i)}_{k|k})}$

$\hat{\mathbf{x}}^{(i)}_k = \mathbf{f}_k(\hat{\mathbf{x}}^{*(i)}_{k|k})$

$P^{(i)}_k = F_k P^{*(i)}_{k|k} F_k^T$

end for

A. SOGs review

Any pdf $p(\mathbf{x})$ can be approximated by a sum of gaussians [6]:

$$\hat{p}(\mathbf{x}) = \sum_{i=1}^{n} w^{(i)} N(\mathbf{x}; \bar{\mathbf{x}}^{(i)}, P^{(i)}) \tag{16}$$

where $\sum_{i=1}^{n} w^{(i)} = 1$, $w^{(i)} \geq 0$.

If the number of terms n increases and the covariances $P^{(i)}$ tend to zero, $\hat{p}(\mathbf{x})$ converges uniformly to $p(\mathbf{x})$.

The prediction and update steps of the SOGs filter are based on the corresponding steps of the EKF for each of the gaussians [6]. Thus, by managing a bank of EKFs the posterior can be properly approximated. The accuracy of the approximation depends on the relation between the degree of uncertainty each gaussian represents and the degree of local nonlinearity of the functions that are approximated by the corresponding step of the EKF.

The actualization of the importance weights $w^{(i)}_k$ can be calculated from:

$$w^{(i)}_k = \frac{w^{(i)}_{k-1} N(\mathbf{z}_k; \mathbf{h}_k(\mathbf{x}^{(i)}_k), S^{(i)}_k)}{\sum_j w^{(j)}_{k-1} N(\mathbf{z}_k; \mathbf{h}_k(\mathbf{x}^{(j)}_k), S^{(j)}_k)} \tag{17}$$

where $S^{(i)}_k$ is the innovation covariance matrix of the gaussian i at instant k. To speed up the process, after each iteration, gaussians with negligible weights can be eliminated.

Using the equations described in section II, the robocentric implementation of the SOGs for the problem proposed is given by algorithm 1

B. Initialization of the Gaussians

Using the first magnetic field measurement ${}^{G_1}\mathbf{z}_1$ expressed in geographic coordinates we can calculate the minimum and

Algorithm 2 : Vanilla Particle Filter.

for $i = 1$ to N **do**
  sample from $\mathbf{x}_{k|k-1}^{(i)} \sim p(\mathbf{x}_k|\mathbf{x}_{k-1}^{(i)}, {}^{R_{k-1}}\mathbf{x}_{R_k})$
  $w^{(i)} = p(\mathbf{z}_k|\mathbf{x}_{k|k-1}^{(i)})$
end for
for $i = 1$ to N **do**
  draw $\mathbf{x}_{k|k}^{(i)}$ from $\{\mathbf{x}_{k|k-1}^{(j)}\}$ with probability $\propto w^{(j)}$
end for

maximum range at which the transmitter can be located [2]:

$$r_{min} = \left(\frac{m_{min}}{4\pi|{}^{G_1}\mathbf{z}_1|}\right)^{\frac{1}{3}} \qquad r_{max} = \left(\frac{2 \cdot m_{max}}{4\pi|{}^{G_1}\mathbf{z}_1|}\right)^{\frac{1}{3}}$$

It is also known [9] that the burial depth of avalanche victims is less than $3m$ in 95% of the cases. Using both results, the transmitter can be located in any position ${}^{G_1}\mathbf{p}_{T_1}$ inside a cylinder ring around the receiver. In order to approximate a uniform distribution, this region is covered by a set of Gaussians. The orientation component ${}^{G_1}\mathbf{\Psi}_{R_1}^{(i)}$ of each gaussian is initialized with the initial misalignment between G_1 and R_1 frames. The value of ${}^{G_1}\mathbf{m}_{T_1}$ is computed using the measured value $\mathbf{z}_1$ and equation (12). All gaussians are given the same initial weight $w_i = 1/n$, where n is the total number of gaussians.

C. Search Control

The mean and covariance of the SOGs distribution are easily calculated from the mean and covariance of its Gaussian components [10]:

$$\begin{aligned} \bar{\mathbf{x}} &= \sum_{i=1}^{n} w^{(i)}\bar{\mathbf{x}}^{(i)} \\ P_x &= \sum_{i=1}^{n} w^{(i)}\{P^{(i)} + (\bar{\mathbf{x}} - \bar{\mathbf{x}}^{(i)})(\bar{\mathbf{x}} - \bar{\mathbf{x}}^{(i)})^T\} \end{aligned} \quad (18)$$

where $\bar{\mathbf{x}}^{(i)}$ and $P^{(i)}$ are the mean and covariance of the ith Gaussian.

The automatization of the searching algorithm is as follows. Initially, the rescuer is directed to follow the direction of the magnetic flux lines. When the receiver position is far enough (in terms of mahalanobis distance) from the mean of the SOGs distribution, the rescuer is directed towards this mean.

IV. Particle Filter

To compare with the SOGs approach we have also developed a particle filter solution that also uses the robocentric representation. In this case, the composition is not postponed because the particle filter can deal with nonlinear functions without approximations. After the first magnetic field measurement, an initial set of particles is generated in a similar way to the one described in III-B. Next, a vanilla particle filter that samples the complete state vector $\mathbf{x}_k$ can be used (algorithm 2). However, the results obtained are extremely poor. The main reason seems to be related to the ${}^{G_k}\mathbf{m}_{T_1}$ component of the state vector, that is a static parameter as shown by equation (8). As it is known, particle filters require process noise to maintain particle diversity after the resampling step. Otherwise the filter will suffer from particle deprivation [11]. We have tried to add an artificial process noise to the parameter ${}^{G_k}\mathbf{m}_{T_1}$, as proposed by [12], without significant improvements on the filter performance.

Algorithm 3 : Rao-Blackwellized Particle Filter.

for $i = 1$ to N **do**
  sample from
  $\mathbf{\Psi}_{k|k-1}^{(i)}, \mathbf{p}_{k|k-1}^{(i)} \sim p(\mathbf{\Psi}_k, \mathbf{p}_k|\mathbf{\Psi}_{k-1}^{(i)}, \mathbf{p}_{k-1}^{(i)}, {}^{R_{k-1}}\mathbf{x}_{R_k})$
  $\hat{\mathbf{z}}_k^{(i)} = \mathbf{h}_k(\mathbf{\Psi}_{k|k-1}^{(i)}, \mathbf{p}_{k|k-1}^{(i)}, \hat{\mathbf{m}}_{k-1}^{(i)})$
  $H_{m_k} = \frac{\partial \mathbf{h}_k}{\partial \mathbf{m}_k}\Big|_{(\hat{\mathbf{m}}_{k-1}^{(i)})}$
  $K_k = M_{k-1}^{(i)} H_{m_k}^T (H_{m_k} M_{k-1}^{(i)} H_{m_k}^T + R_k)^{-1}$
  $\hat{\mathbf{m}}_k^{(i)} = \hat{\mathbf{m}}_{k-1}^{(i)} + K_k(\mathbf{z}_k - \hat{\mathbf{z}}_k^{(i)})$
  $M_k^{(i)} = (I - K_k H_{m_k}) M_{k-1}^{(i)}$
  $w_k^{(i)} = \eta\ w_{k-1}^{(i)}\ N(\mathbf{z}_k; \hat{\mathbf{z}}_k^{(i)}, H_{m_k} M_{k-1}^{(i)} H_{m_k}^T + R_k)$
end for
for $i = 1$ to N **do**
  draw $\mathbf{\Psi}_{k|k}^{(i)}, \mathbf{p}_{k|k}^{(i)}$ from $\{\mathbf{\Psi}_{k|k-1}^{(j)}, \mathbf{p}_{k|k-1}^{(j)}\}$ with probability $\propto w_k^{(j)}$
end for

We have developed a second implementation based on a Rao-Blackwellized particle filter [7] following a derivation similar to the proposed in the FastSLAM [13]. Using this technique the posterior is factorized into two probabilities:

$$\begin{aligned} p(\mathbf{x}^k|\mathbf{z}^k, \mathbf{u}^k) &= p(\mathbf{\Psi}^k, \mathbf{p}^k, \mathbf{m}|\mathbf{z}^k, \mathbf{u}^k) \\ &= p(\mathbf{m}|\mathbf{\Psi}^k, \mathbf{p}^k, \mathbf{z}^k, \mathbf{u}^k) p(\mathbf{\Psi}^k, \mathbf{p}^k|\mathbf{z}^k, \mathbf{u}^k) \end{aligned} \quad (19)$$

where $\mathbf{u}$ represents the receiver motion and the superscript k means the data obtained up to time instant k. The first part, corresponding to the magnetic moment, will be estimated with a Kalman filter whereas the rest of the state vector will be estimated with a particle filter (algorithm 3). For each particle, the initial value for $\mathbf{m}$ will be computed from the first measurement of the magnetic field using equation (12). Notice the linear relation in the measurement equation between $\mathbf{z}$ and $\mathbf{m}$. As a consequence, the estimation of $\mathbf{m}$ with the Kalman filter will be performed without any approximation. The covariance matrix of the magnetic moment $\mathbf{m}$ is denoted by M.

It is important to determine when to carry out the resampling operation in order to reduce the probability of eliminating particles that are near the transmitter. In our case, this is specially true in the initial steps of the searching. The criterion selected is based on the effective sample size $\hat{N}_{eff}$ which determines the approximate number of samples that actually contribute to the estimate [14]. It is defined as

$$\hat{N}_{eff} = \frac{1}{\sum_{i=1}^{N}(w_k^{(i)})^2} \quad (20)$$

The resampling step is performed only when $\hat{N}_{eff}$ is below a given threshold.

The search control implemented to guide the receiver towards the transmitter is similar to the one described in III-C.

V. Results

In this section simulation results obtained with the SOGs and RBPF are studied. Figures 2 and 3 show three snapshots of the performance of both filters for the same problem. In this case, the initial distance between transmitter and receiver is 53 meters. Each edge of the simulated surface represents 10 meters approximately. After the first measurement, gaussians and particles are distributed in a cylinder-ring (left figures). The receiver antenna is located at the center of the ring whereas the transmitter represented by a big arrow is situated on the left. The arrow points in the direction of the magnetic moment of the transmitter antenna. A few steps later (central figures), the posterior pdf is reduced to a smaller region that contains the real location of the transmitter. For the SOGs filter, half of the gaussians have been already eliminated whereas for the RBPF the particles have been concentrate around the transmitter by the resampling step. At this point the rescuer is going straightforward to the victim's location. Right figures show a more advanced step of the search. The uncertainty in the location of the victim has been greatly reduced and the posterior begins to be similar to a single gaussian in both cases.

To analyze the performance of the proposed algorithms 100 tries have been performed. On each try the position, orientation and power of the transmitter is randomly chosen. It is assumed that the receiver is moving at $1m/s$ taking a measurement per second. The initial distance between the rescuer and the transmitter varies from 40 to 60 meters.

The initial number of gaussians used in all the tries is 1700. This number is consecutively reduced during the search. In the final steps, less than 15 gaussians usually survived. In the RBPF 5000 particles are maintained during all the search. For this number of gaussians and particles the algorithms can be implemented in real time and have comparable computing times.

Table I summarizes the results of the 100 tries. The number of steps required to find the transmitter is quite similar in both algorithms. The error rows represent the difference, in meters, between the true victim's location and the estimated location obtained with the SOGs and the RBPF. A more detailed description of these errors are shown on figures 4, 5. As can be appreciated on figure 5, there are 25 tries in the particle filter in which the algorithm has failed in more than 1 meter in the estimation of transmitter location. A supervised run of these cases shows that the filter has suffered from particle deprivation, loosing particles near the real location of the transmitter. To assure robustness, the number of particles can be incremented, but then the time needed is greater than in the gaussian case. Figure 4 shows the errors obtained with the SOGs filter. As can be seen, errors are bounded and mainly distributed in the interval $[0.1, 0.4]$ meters. Therefore, for the implementations explained, the SOGs filter seems to be more robust.

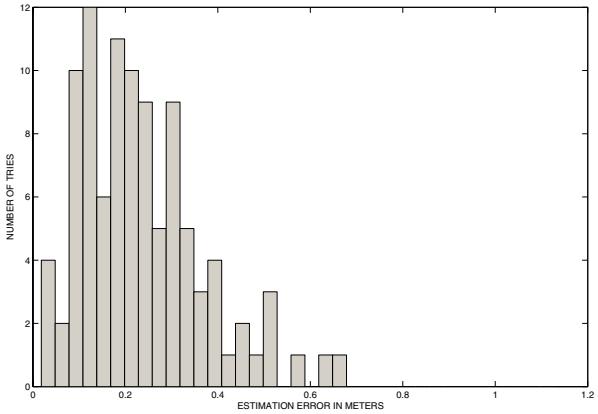

Fig. 4. Distribution of victim localization errors in 100 tries using SOGs filter. Errors are concentrated in the interval $[0.1, 0.4]$ meters.

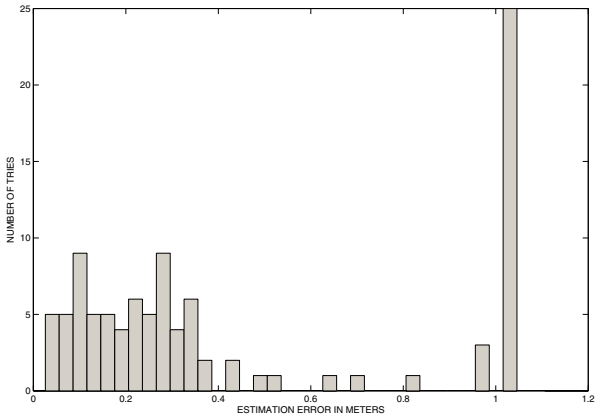

Fig. 5. Distribution of victim localization errors in 100 tries using RBPF. The big bin on the right corresponds to the total number of tries with error bigger than 1 meter.

VI. Conclusions

A robocentric SLAM approach has been implemented in this paper to localize a person buried in the snow by an avalanche. Using this technique the location of the victim is estimated with respect to the current location of the rescuer. With this information, the rescuer can be directly guided to approach and find the victim.

Since the posterior that characterizes the location of the transmitter is multimodal, classical SLAM techniques based

TABLE I
Comparisons between SOG Filter and Rao-Blackwellized Particle Filter

	MAX	MEAN	MEDIAN
SOGs error	0.66	0.23	0.21
RBPF error	32.5	2.27	0.28
Initial receiver distance	60	50.4	51
Steps SOGs	93	62	61
Steps RBPF	99	64	64

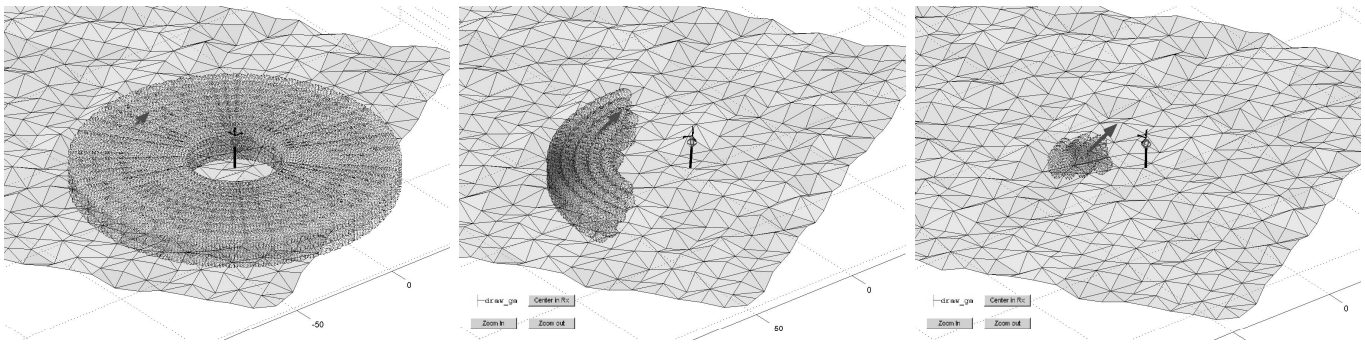

Fig. 2. Initial distribution of the Gaussians in a cylinder-ring (left), After some steps some hypothesis disappear (middle), Gaussians concentrate near the real location of the transmitter (right).

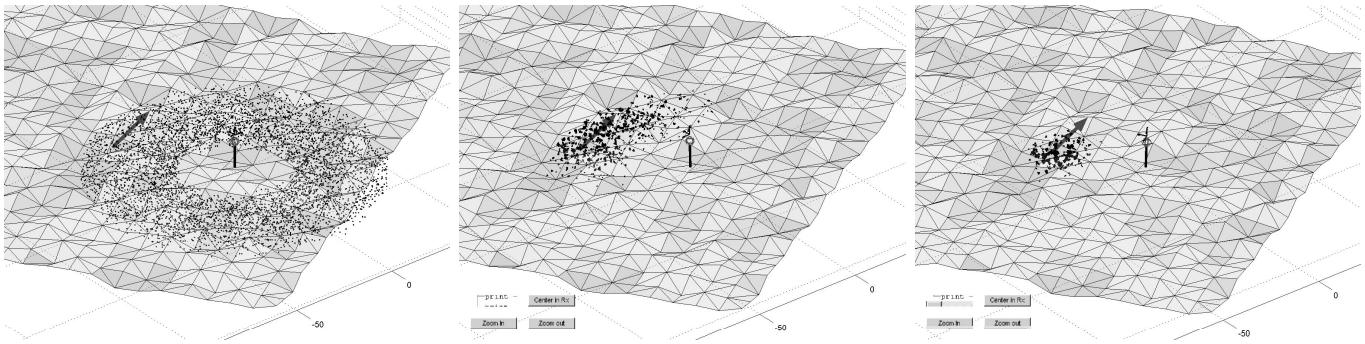

Fig. 3. Initial distribution of the particles in a cylinder-ring (left), After some steps the resampling process distributes particles in the vicinity of the transmitter (middle), Particles concentrate near the real location of the transmitter (right).

on Kalman Filter cannot be directly applied. Instead two alternative solutions based on SOGs filter and particle filter are proposed.

In both algorithms, the victim is localized in a comparable number of steps. However, for the implementations proposed, the SOGs filter seems to be more robust and accurate in the estimation.

Future work will study improvements of the SOGs filter. The problem of finding several victims and the best trajectory of the rescuer to reduce their uncertainty localization will be also addressed.

ACKNOWLEDGMENTS

This research has been funded in part by the Dirección General de Investigación of Spain under project DPI2003-07986.

REFERENCES

[1] M. Falk, H. Brugger, and L. Kastner, "Avalanche survival chances," *The Newsletter of the International Society for Mountain Medicine*, vol. 4, 1994.

[2] P. Piniés and J. D. Tardós, "Fast localization of avalanche victims using sum of gaussians," in *IEEE Int. Conf. on Robotics and Automation*, Orlando, Florida, 2006, to appear.

[3] J. A. Castellanos and J. D. Tardós, *Mobile Robot Localization and Map Building: A Multisensor Fusion Approach*. Boston, Mass.: Kluwer Academic Publishers, 1999.

[4] M. W. M. G. Dissanayake, P. Newman, S. Clark, H. F. Durrant-Whyte, and M. Csorba, "A solution to the simultaneous localization and map building (SLAM) problem," *IEEE Trans. on Robotics and Automation*, vol. 17, no. 3, pp. 229–241, 2001.

[5] J. Castellanos, J. Neira, and J. Tardós, "Limits to the consistency of EKF-based SLAM," in *5th IFAC Symposium on Intelligent Autonomous Vehicles*, Lisbon, Portugal, 2004.

[6] D. L. Alspach and H. W. Sorenson, "Nonlinear bayesian estimation using gaussian sum approximations," *IEEE Transactions on Automatic Control*, vol. AC-17, pp. 439–448, 1972.

[7] A. Doucet, N. de Freitas, K. Murphy, and S. Russell, "Rao-blackwellised particle filtering for dynamic bayesian networks," in *Proceedings of Uncertainty in AI (UAI)*, 2000.

[8] R. Smith, M. Self, and P. Cheeseman, "Estimating uncertain spatial relationships in robotics," in *Uncertainty in Artificial Intelligence 2*, J. Lemmer and L. Kanal, Eds. Elsevier Science Pub., 1988, pp. 435–461.

[9] T. Auger and B. Jamieson, "Avalanche probing re-visited," in *International Snow Science Workshop*, Banff, 1996, pp. 295–298.

[10] Y. Bar-Shalom, X. Li, and T. Kirubarajan, *Estimation with Applications to Tracking and Navigation*. New York: John Willey and Sons, 2001.

[11] S. Thrun, W. Burgard, and D. Fox, *Probabilistic Robotics*. The MIT Press, September 2005.

[12] N. J. Gordon, D. Salmond, and C. Ewing, "Novel approach to nonlinear/non-gaussian bayesian state estimation," in *IEE Proceedings-F*, 1993.

[13] M. Montemerlo, S. Thrun, D. Koller, and B. Wegbreit, "FastSLAM: A factored solution to the simultaneous localization and mapping problem," in *Proceedings of the AAAI National Conference on Artificial Intelligence*. Edmonton, Canada: AAAI, 2002.

[14] A. Doucet, N. de Freitas, and N. Gordon, Eds., *Sequential Monte Carlo Methods in Practice*. Springer, 2001.